Supplemental Material for Quantum Sensing with Erasure Qubits

Pradeep Niroula,[1,2] Jack Dolde,[3] Xin Zheng,[3] Jacob Bringewatt,[1,2] Adam Ehrenberg,[1,2] Kevin C. Cox,[4] Jeff Thompson,[5] Michael J. Gullans,[1] Shimon Kolkowitz,[3] and Alexey V. Gorshkov[1,2]

[1] *Joint Center for Quantum Information and Computer Science, NIST/University of Maryland, College Park, Maryland 20742, USA*
[2] *Joint Quantum Institute, NIST/University of Maryland, College Park, Maryland 20742, USA*
[3] *Department of Physics, University of Wisconsin-Madison, Madison, Wisconsin 53706, USA*
[4] *DEVCOM Army Research Laboratory, Adelphi, Maryland 20783, USA*
[5] *Department of Electrical and Computer Engineering, Princeton University, Princeton, NJ, 08544, USA*

(Dated: June 10, 2024)

In this Supplemental Material, we elaborate on the computation of the Fisher information for the case of sensing using a single qubit subject to dephasing or depolarizing noise (Section S1) and demonstrate the claim in the main text that the optimal single-qubit probe state remains unchanged in these settings relative to the noiseless case (Section S2). We also extend our discussion of erasure errors from the case of a single qubit to multi-qubit ensembles subject to both global and local depolarizing and dephasing noise channels (Section S3). Finally, we describe additional details of the experimental implementation (Section S4).

S1. DEPOLARIZING AND DEPHASING NOISE

In this section, we describe in more detail how the Fisher information for single-qubit sensing subject to either dephasing or depolarizing noise depends on the noise strength.

Recall that, in the main text, we began by considering the simplest form of noise where random single-qubit Pauli operators act on the sensor with equal probability $q/4$. This gives rise to a depolarizing noise model of strength q with $\mathcal{E}_\phi(\rho_0) = \mathbb{1}/2$. In Section S2, we will show that the optimal input state for sensing under depolarizing noise is the same as for sensing without noise—that is, $\rho_0 = |+\rangle\langle+|$. If we measure the final state in some general basis given by $|\pm\theta\rangle = (|0\rangle \pm e^{i\theta}|1\rangle)/\sqrt{2}$, the corresponding Fisher information, for this choice of measurement basis, is given by

$$\mathcal{F}_{\text{depol}} = \left\langle \left(\frac{\partial \log p_x}{\partial \phi} \right)^2 \right\rangle_{x\in\{+,-\}} = \frac{(1-q)^2 \sin^2(\phi-\theta)}{1-(1-q)^2\cos^2(\phi-\theta)}. \tag{S1}$$

Thus, choosing ϕ-dependent basis achieves the maximum Fisher information of $(1-q)^2$ [S1]. As having such prior information about the unknown parameter value is unrealistic, the achievable Fisher information is usually lower than the maximal value of $(1-q)^2$.

Alternatively, if we assume that the noise channel can only impart a phase-flip during the sensing process with probability q, we get a dephasing noise of the form $\mathcal{E}_\phi[\rho_0] = \sigma_z\rho_\phi\sigma_z$ with $\rho_\phi = \exp(-i\phi\sigma_z/2)\,\rho_0\exp(i\phi\sigma_z/2)$. For the single-qubit sensing problem we consider here subject to such dephasing, noise we have the map

$$\rho_0 \to (1-q)\rho_\phi + q\sigma_z\rho_\phi\sigma_z = (1-2q)\rho_\phi + (2q)\frac{\mathbb{1}}{2}, \tag{S2}$$

which is the same as a depolarizing noise model with a modified strength $q \to 2q$. Dephasing and depolarizing noise are often used to model realistic quantum devices [S2, S3]. In both of these cases, the Fisher information scales quadratically in $(1-q)$, meaning we fail to saturate the linear in $(1-q)$ bound dictated by the convexity [S1].

S2. OPTIMAL INPUT STATES FOR NOISY SENSING

In this section, we show that the optimal input state for noisy sensing of a single parameter under depolarizing noise is the same as that for noiseless sensing.

Consider a single-qubit input state, ρ_0, which evolves under the sensing unitary $U_\phi = \exp(i\phi H)$, with ϕ being the unknown parameter we want to sense and H being the generator Hamiltonian. The quantum Fisher information, as a function of the input state ρ_0, with respect to the parameter ϕ, is given by Ref. [S4]

$$\mathcal{F}(\rho_0) = 4(2\,\text{tr}(\rho_0^2) - 1)|\langle\lambda_0|H|\lambda_1\rangle|^2, \tag{S3}$$

where λ_0 and λ_1 are the eigenvectors of ρ_0. Because the depolarizing channel and the unitary channel commute, we let the unitary act noiselessly on a depolarized input state, which is given by

$$\tilde{\rho}_0 = (1-q)\rho_0 + q\frac{\mathbb{1}}{2}, \tag{S4}$$

where q is the depolarization strength. Noting that the eigenstates of $\tilde{\rho}_0$ and ρ_0 are the same, Eq. (S3) evaluates to

$$\mathcal{F}(\tilde{\rho}_0) = (1-q)^2\mathcal{F}(\rho_0). \tag{S5}$$

Note that the above expression is generically true for all input states ρ_0, meaning that the effect of noise is to simply scale the Fisher information by $(1-q)^2$, regardless of the input state. Therefore, the optimal state to use for noisy sensing is the same as that for noiseless sensing.

S3. MULTI-QUBIT ERASURES

In this section, we extend our comparison of erasure error with other types of errors to multi-qubit ensembles. We focus on two cases, one where qubits in the ensemble are unentangled and another where the ensemble qubits are fully entangled. We show that, in both cases, erasure qubits retain their metrological advantage.

Unentangled ensemble

Consider an experiment with n unentangled spins, each initialized in the $|+\rangle$ state, and each evolving under the sensing Hamiltonian $\exp(-i\phi\sigma_z/2)$, such that the multi-qubit ensemble takes the tensorized form $\rho_\phi^{\otimes n} = (|\psi(\phi)\rangle\langle\psi(\phi)|)^{\otimes n}$ with $|\psi(\phi)\rangle = (e^{i\phi/2}|0\rangle + e^{-i\phi/2}|1\rangle)/\sqrt{2}$.

The extractable information about the unknown parameter ϕ depends on the choice of measurement we make on the ensemble, which can be a general positive-operator valued measure (POVM). The maximum information obtained by optimizing over all possible POVMs is given by the quantum Fisher information (QFI). For product states, the QFI is additive: $\mathcal{F}(\rho^{\otimes n}) = n\mathcal{F}(\rho)$. Therefore, for the unentangled ensemble, the QFI of the entire ensemble of spins is n times the QFI of a single spin.

Consequently, the QFIs for an ensemble that undergoes depolarizing noise and erasure noise are $n(1-q)^2$ and $n(1-q)$, respectively, where we have borrowed the single-spin QFI from the main text. For both types of noise, the Fisher information scales with n, implying that the standard deviation in the estimator of ϕ scales, following the Cramér-Rao bound, as $1/\sqrt{n}$.

Entangled ensemble

Now, we consider the case of a fully-entangled ensemble. More specifically, we consider the multi-qubit sensor state given by the GHZ state $\left(|0\rangle^{\otimes n} + |1\rangle^{\otimes n}\right)/\sqrt{2}$, which, in the absence of noise, evolves to $\rho_\phi = |\psi_\phi^n\rangle\langle\psi_\phi^n|$ with $|\psi_\phi^n\rangle = \left(e^{-in\phi/2}|0\rangle^{\otimes n} + e^{in\phi/2}|1\rangle^{\otimes n}\right)/\sqrt{2}$. This is the optimal probe state for noiseless sensing under the given Hamiltonian.

For a generic mixed probe state ρ we may calculate the QFI under a unitary encoding of the parameter ϕ by calculating the eigenvalues λ_i and the eigenvectors $|\lambda_i\rangle$ of ρ and evaluating the following expression [S4]:

$$\mathcal{F} = \sum_{\substack{k,l \\ \lambda_k+\lambda_l\neq 0}} \frac{2\cdot|\langle\lambda_k|\partial_\phi\rho|\lambda_l\rangle|^2}{\lambda_k+\lambda_l} = \sum_{\substack{k,l \\ \lambda_k+\lambda_l\neq 0}} \frac{2\cdot|\langle\lambda_k|i(A\cdot\rho-\rho\cdot A)|\lambda_l\rangle|^2}{\lambda_k+\lambda_l} = \sum_{\substack{k,l \\ \lambda_k+\lambda_l\neq 0}} \frac{2\cdot(\lambda_k-\lambda_l)^2}{\lambda_k+\lambda_l}|\langle\lambda_k|A|\lambda_l\rangle|^2. \tag{S6}$$

Above, we have used the fact that $\partial_\phi\rho = \partial_\phi\left(e^{-i\phi A}\cdot\rho_0\cdot e^{i\phi A}\right) = -i(A\cdot\rho-\rho\cdot A)$, where ρ_0 is the initial sensing state, and A is the generator corresponding to the sensing process. In the case of multi-qubit sensing, where the unknown parameter ϕ couples to each of the sensors via a $\sigma_z/2$ operator, we have $A = \sum_{i=1}^n \sigma_z^{(i)}/2$, where $\sigma_z^{(i)}$ indicates that the operator acts on qubit i (with identity on the rest of the qubits).

For ease of exposition, we first consider the case where the noise acts globally. The depolarizing noise takes the state to a globally depolarized or fully-mixed state, that is

$$\rho_\phi \to \tilde{\rho}_\phi = (1-q)\rho_\phi + q\frac{\mathbb{1}_n}{2^n}, \tag{S7}$$

and the erasure error takes the state to a global erasure state, which we denote by $\rho_\perp$, that is

$$\rho_\phi \to \tilde{\rho}_\phi = (1-q)\rho_\phi + q\rho_\perp. \tag{S8}$$

A global erasure state is a state that is outside the sensing subspace and is detectable without affecting the sensing space. For example, consider a GHZ state and a noise channel consisting only of an odd number of bit-flips. Measuring the parity of the state will reveal the occurrence of the error. As a result, the entire subspace of odd parity can be considered a global erasure state.

We now compute the Fisher information corresponding to the depolarizing and erasure channels by considering the eigenvalues in Eq. (S7) and Eq. (S8), respectively. As the noiseless state ρ_ϕ has only one non-zero eigenvalue, in the noiseless case, the sum in Eq. (S6) only includes one term. With the addition of depolarizing noise, the eigenvalues of the depolarized noisy state include contributions from the maximally mixed state: one eigenvalue is $(1-q)+q/2^n$ (with eigenvector $|+_\phi\rangle = (e^{-in\phi/2}|0\rangle^{\otimes n} + e^{in\phi/2}|1\rangle^{\otimes n})/\sqrt{2}$) and the rest are $q/2^n$ (with eigenvectors $\{|-_\phi\rangle = (e^{-in\phi/2}|0\rangle^{\otimes n} - e^{in\phi/2}|1\rangle^{\otimes n})/\sqrt{2}\} \cup \{|\hat{e}_k\rangle\}_{k\in[2,2^n-1]}$, where $|\hat{e}_k\rangle$ runs over the 2^n-2 computational basis states other than $|0\rangle^{\otimes n}$ and $|1\rangle^{\otimes n}$. The non-zero contributions to Eq. (S6) come from two choices of k and l, when $|\lambda_k\rangle = |+_\phi\rangle$ and $|\lambda_l\rangle = |-_\phi\rangle$ (and vice versa). For each of the two terms, we have $|\lambda_k - \lambda_l| = (1-q)$, $\lambda_k + \lambda_l = q\cdot 2^{1-n} + (1-q)$ and $|\langle\lambda_k|A|\lambda_l\rangle| = n/2$. Therefore, we obtain

$$\mathcal{F}^{\text{depol}} = \frac{n^2\cdot(1-q)^2}{q\cdot 2^{1-n} + (1-q)}. \tag{S9}$$

For erasure error, the inclusion of the erasure state $\rho_\perp$ introduces eigenvectors that are orthogonal to the eigenvectors of the noiseless state ρ_ϕ. The non-zero contributions to Eq. (S6) come from two choices of k and l, when $|\lambda_k\rangle = |+_\phi\rangle$ and $|\lambda_l\rangle = |-_\phi\rangle$ with eigenvalues $\lambda_k = 1-q$ and $\lambda_l = 0$ (and vice versa), such that the Fisher information evaluates to

$$\mathcal{F}^{\text{erasure}} = n^2(1-q). \tag{S10}$$

Note that, in the limit $n\to\infty$, we get

$$\lim_{n\to\infty} \mathcal{F}^{\text{depol}} = \mathcal{F}^{\text{erasure}}. \tag{S11}$$

We explain this limit as follows: the depolarizing noise takes the state to a maximally mixed state which has an exponentially small overlap with the original codespace. If we can engineer complicated non-local measurements, we can detect if the state has left the sensing subspace defined by the GHZ state. While this erasure-detection measurement is easy for an erasure state, this can be extremely difficult to engineer for a generic depolarized state.

Crucially, such a limit does not hold for arbitrary noise. For example, consider the global dephasing noise

$$\rho_\phi \to (1-q)\rho_\phi + qZ^{\otimes n}\rho_\phi Z^{\otimes n}, \tag{S12}$$

where $Z = -i\exp(i\pi\sigma_z/2)$. We have $Z^{\otimes n}\rho_\phi Z^{\otimes n} = \rho_{\phi+n\pi}$; the dephasing error keeps the sensor within the sensing codespace. For even n, global dephasing noise has no effect on the ensemble, that is, $\rho_{\phi+n\pi} = \rho_\phi$ for even n. However, for odd n, this state has a QFI given by

$$\mathcal{F}^{\text{dephas}} = n^2(1-q)^2, \tag{S13}$$

which does not have an asymptotic limit that tends to the Fisher information corresponding to erasure noise.

While we considered the effects of global noise in the analysis above, a more realistic noise model would include local noise acting independently on all qubits in the ensemble. For local depolarizing and local erasure noise, the noise model would look like

$$\rho_\phi \to \sum_{\boldsymbol{k}\in\{0,1\}^n} (1-q)^{n-|\boldsymbol{k}|}q^{|\boldsymbol{k}|}\,\text{tr}_{\boldsymbol{k}}(\rho_\phi)\otimes\mathcal{E}^{\otimes|\boldsymbol{k}|}, \tag{S14}$$

where we sum over all possible combinations of errors in n qubits, $|\boldsymbol{k}|$ denotes the Hamming weight of the binary vector $\boldsymbol{k}$, $\text{tr}_{\boldsymbol{k}}(\rho)$ denotes the reduced density matrix obtained by tracing out qubits on which the noise acts, and $\mathcal{E}^{\otimes|\boldsymbol{k}|}$ denotes the local error on qubits defined $\boldsymbol{k}$. For local depolarizing noise, $\mathcal{E} = \mathbb{1}/2$, and for local erasure noise, $\mathcal{E} = |\perp\rangle\langle\perp|$, where $|\perp\rangle$ is the local erasure state on each individual sensor. For local dephasing noise, the noise model is instead given by

$$\rho_\phi \to \sum_{\boldsymbol{k}\in\{0,1\}^n} (1-q)^{n-|\boldsymbol{k}|}q^{|\boldsymbol{k}|}Z^{\boldsymbol{k}}\cdot\rho_\phi\cdot Z^{\boldsymbol{k}}, \tag{S15}$$

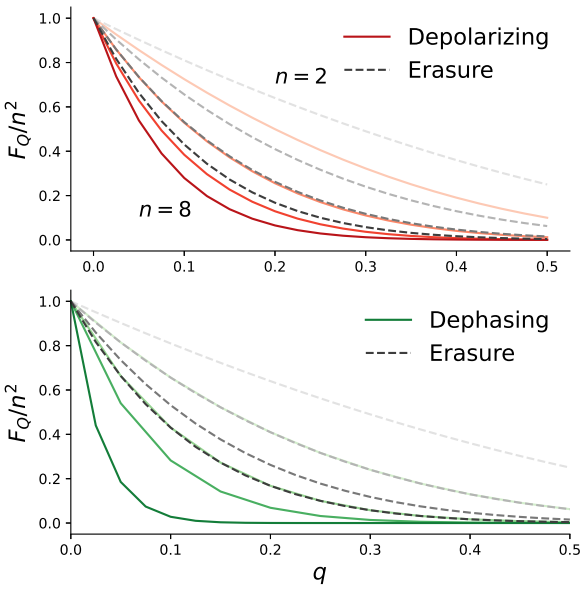

FIG. S1. Quantum Fisher information with local independent depolarizing (red solid lines), dephasing (green solid lines), and erasure (gray dashed lines) noise for n between two (lightest shade) and eight (darkest shade). The QFI for depolarizing noise approaches the QFI for erasure noise for large n.

where $Z^{\boldsymbol{k}}$ denotes a composite Pauli operator with Z operators in position i whenever $k_i = 1$ and identity operator otherwise.

We can evaluate the QFI of these noise processes for different q and different n numerically. The results are plotted in Fig S1. We observe that, similar to the global noise model, erasure error has the largest QFI, and the QFI for depolarizing noise approaches the QFI for erasure at large n.

S4. EXPERIMENTAL IMPLEMENTATION

In this section, we provide additional details on various aspects of the experimental demonstration of our results.

Sample preparation

In order to measure the impact of erasure and dephasing errors on a quantum system, we perform differential measurements of two spatially-resolved ensembles of ^{87}Sr atoms loaded into a one-dimensional (1D) optical lattice. To prepare the atomic sample, we use a standard two-stage magneto-optical trap (MOT) technique based on the broad-linewidth ($\approx$ 30 MHz) $^1S_0$ - $^1P_1$ transition at 461 nm and the narrow-linewidth ($\approx$ 7.5 kHz) $^1S_0$ - $^3P_1$ transition at 689 nm. These trapped atoms are then transferred to a 1D optical lattice, which is created through a retro-reflected laser beam tuned to the "magic" wavelength at 813 nm.

To prepare two atomic ensembles, we first load atoms from the 689 nm MOT into one region of the lattice for roughly 20 ms. The 689 nm MOT is then displaced along the lattice propagation axis by adjusting the current in the MOT coils to shift the location of the magnetic field zero, and a second region of the lattice is loaded for about 25 ms to achieve roughly equal atom numbers. The separation between the two ensembles used in the data shown in Fig. 2 of the main text is approximately 0.8 mm.

Hyperfine state initialization

Following loading into the lattice from the MOT, we spin polarize the atoms into the stretched state $|^1S_0, m_F = +9/2\rangle$, followed by in-lattice cooling on the $^1S_0$ - $^3P_1$ transition both axially (sideband cooling) and radially (Doppler cooling). We then initialize the sample into our desired hyperfine state $|e, m_F = +3/2\rangle$ through three successive σ^- transitions

through the ground ($^1S_0$, g) and clock ($^3P_0$, e) states hyperfine manifold, i.e. $|g, m_F = +9/2\rangle \rightarrow |e, m_F = +7/2\rangle$, $|e, m_F = +7/2\rangle \rightarrow |g, m_F = +5/2\rangle$, and $|g, m_F = +5/2\rangle \rightarrow |e, m_F = +3/2\rangle$. Each clock pulse is followed by a "clean-up" pulse on the $^1S_0$ - $^1P_1$ transition ($^3P_0$ - $^3S_1$ and $^3P_2$ - $^3S_1$ transitions) to remove any residual atoms in the ground (clock) state.

Synchronous Ramsey interrogation

We perform synchronous Ramsey differential measurements on the $|g, m_F = +5/2\rangle \leftrightarrow |e, m_F = +3/2\rangle$ transition, consisting of an initial $\pi/2$ pulse, followed by a period (T) of no laser light, referred to as Ramsey interrogation time or Ramsey dark time, and a final $\pi/2$ pulse. The synchronous Ramsey technique we employ in this work uses 2 atomic ensembles interrogated simultaneously with a shared clock laser beam along the lattice axis, as shown in Fig. 2(a) and (b) of the main text. The populations in the ground and excited clock states of two ensembles are read out in parallel with imaging pulses along the lattice axis, with scattered photons collected on a camera (Andor, iXon-888). The excitation fraction is extracted through $P = (N_e - N_{bg})/(N_g + N_e - 2N_{bg})$, where N_g, N_e, and N_{bg} are the ground state population, excited clock state population, and background counts without atoms, respectively.

Because the free evolution time T (8 s) is orders of magnitude longer than the local oscillator coherence time (about 100 ms), the phase of the final $\pi/2$ pulse is random. The excitation fraction of these two ensembles (P_0 and P_1) can be written as

$$\begin{aligned} P_0 &= \frac{1}{2}(1 + C_0 \cos(\theta_l)), \\ P_1 &= \frac{1}{2}(1 + C_1 \cos(\theta_l + \phi_d)), \end{aligned} \tag{S16}$$

where C_0 and C_1 are the respective contrasts of each ensemble, θ_l is the random laser phase, and ϕ_d is a fixed relative phase. When the excitation fractions from the two regions are plotted parametrically, the data traces out an ellipse due to the fixed relative phase between the Ramsey fringes of the two ensembles. The relative phase can then be extracted through a least-squares fit to the ellipse, as detailed in our previous work [S5]. To extract the stability of the measured relative phase between the ensembles, we use a jackknifing technique [S6] to construct an Allan deviation, which can be fit with a slope corresponding to a white noise model due to laser frequency noise. To extract the contrast, we use the variance of the measured excitation fraction for each ensemble given as

$$C_i = 1 - \left| 1 - \sqrt{8\sigma_i^2} \right|. \tag{S17}$$

The final contrast is then given as the average of the two ensembles.

Lattice-induced dephasing

Due to radial motion within the 1D optical lattice, trapped atoms experience a varying lattice intensity as they sample the Gaussian profile of the laser beam. This results in ac Stark shifts of both the ground and excited states of the atom based on its radial motion within the lattice potential. At the 'magic wavelength', the polarizabilities of the ground and excited states are equal such that the trapping light causes an equal, at least to leading order, shift in the energies of the ground and excited states. As we detune from the magic wavelength in this experiment, the dephasing error rate increases due inhomogeneous broadening from the radial motion, which manifests as a reduced contrast of the ellipses from the synchronous Ramsey comparisons. To perform the measurements shown in Fig. 2 of the main text, we use a TiSapphire laser (Matisse C from Sirah) at 368.55486(1) THz, corresponding to our operational magic wavelength, that is frequency locked to a wavemeter with an accuracy of approximately 10 MHz. In the measurements show in Fig. 2(g) of the main text, we detune a maximum of 2.0 GHz away from the magic wavelength, which corresponds to a contrast of 0.21(3).

[S1] J. Kołodyński and R. Demkowicz-Dobrzański, New J. Phys. **15**, 073043 (2013).
[S2] P. Krantz, M. Kjaergaard, F. Yan, T. P. Orlando, S. Gustavsson, and W. D. Oliver, Appl. Phys. Rev. **6** (2019).
[S3] M. A. Nielsen and I. L. Chuang, *Quantum Computation and Quantum Information* (Cambridge University Press, 2010).
[S4] J. Liu, H. Yuan, X.-M. Lu, and X. Wang, J. Phys. A **53**, 023001 (2020).

[S5] X. Zheng, J. Dolde, M. C. Cambria, H. M. Lim, and S. Kolkowitz, Nat. Commun. **14**, 4886 (2023).
[S6] G. E. Marti, R. B. Hutson, A. Goban, S. L. Campbell, N. Poli, and J. Ye, Phys. Rev. Lett. **120**, 103201 (2018).